

The SCE_xAO NIR Speckle Lifetime Experiment

Sean B. Goebel^{a,b}, Olivier Guyon^{b,c,d,e}, Donald N.B. Hall^a, and Nemanja Jovanovic^{b,f}

^aInstitute for Astronomy, University of Hawaii, 640 North A’ohoku Place, Hilo, HI 96720

^bSubaru Telescope, National Astronomical Observatory of Japan, 650 North A’ohoku Place, Hilo, HI 96720

^cSteward Observatory, University of Arizona, Tucson, AZ 85721

^dCollege of Optical Sciences, University of Arizona, Tucson, AZ 85721

^eAstrobiology Center of NINS, 2-21-1, Osawa, Mitaka, Tokyo, 181-8588, Japan

^fDepartment of Physics and Astronomy, Macquarie University, Sydney, NSW 2109, Australia

ABSTRACT

We describe in this paper an experiment to predict the performance of a real-time speckle nulling loop using high frame rate speckle images collected using a SAPHIRA detector on the SCE_xAO instrument. Even after extreme adaptive optics corrections, a halo of speckles surrounds the PSF core, and these speckles must be mitigated in order to detect faint structures such as disks or extrasolar planets. Several post-processing techniques such as ADI, PDI, and SDI enable the differentiation between speckles and intrinsic features in the science target, but their ability to improve contrast is limited. In order to detect faint objects such as reflected-light exoplanets, additional techniques need to be implemented. A promising technique is speckle nulling, whereby artificial speckles are generated on top of speckles in the halo in order to destructively interfere them away. If such a loop is implemented with high temporal bandwidth on-sky, then both static and rapidly-changing speckles could be reduced, enabling greatly improved contrasts. We collected 1.7 kHz H-band images and are in the process of analyzing them to simulate the performance of such a loop.

Keywords: Extreme adaptive optics, SCE_xAO, SAPHIRA, speckles, high-contrast imaging

1. INTRODUCTION

Extreme adaptive optics (AO) images consist of a point spread function (PSF) and a surrounding halo of speckles. The PSF’s size is determined by the diffraction limit of the telescope, and the speckle halo has an angular size corresponding to that of the natural atmospheric seeing. The speckle halo is composed of speckles with intensities up to a few 10^{-3} times the intensity of the PSF core. The speckles are caused by diffraction within the optical train and imperfect AO corrections due to time lag between wavefront sensing and correction, chromatic differences between the wavefront sensor and science camera, or imperfect wavefront measurements due to noise. These speckles evolve on a variety of timescales, from static (caused by diffraction from the telescope spiders, for example) to millisecond (the deformable mirror update rate).¹

These speckles reduce the ability to detect faint features near a star such as extrasolar planets or debris disks. Several techniques have been developed to differentiate between speckles and actual structure in the science object. These include angular differential imaging² (which takes advantage of the rotation of the sky relative to an alt/az telescope) and spectral differential imaging³ (which utilizes the fact that the speckle halo expands with increasing wavelengths, but features in the target do not). However, because these techniques are implemented after the data has been collected, they do not remove the shot noise caused by the speckles. Additionally, because they are typically applied to long exposures, they have no effect on quickly-changing speckles. These techniques have been applied to obtain contrasts on the order of 10^{-6} at several tenths of an arcsecond from the PSF core. However, an Earth-like planet around a Sun-like star has a contrast of 10^{-10} , so better speckle reduction strategies need to be implemented if such planets are to be detected.

Send correspondence to Sean Goebel, sgoebel@ifahawaii.edu

Various techniques have been proposed for real-time speckle nulling loops.^{4,5} These provide two advantages over post facto speckle mitigation techniques such as those discussed above. First, they are able to reduce some of the dynamic speckles in addition to the static ones. The loop’s temporal bandwidth determines to what extent the short-lived speckles can be reduced. Second, because a real-time speckle nulling loop utilizes interferometry, it removes both the speckles and their shot noise.

However, the temporal bandwidths of the few speckle nulling loops that have been implemented have been relatively slow. In this paper, we describe an experiment which aims to utilize high frame rate SAPHIRA speckle data in order to predict the performance of a high-speed speckle nulling loop.

2. EXPERIMENTAL SETUP AND DATA COLLECTION

2.1 The Speckle Nulling Loop Algorithm, SCEXAO, and the SAPHIRA Detector

Martinache et al.⁶ implemented a simple and robust speckle nulling loop on SCEXAO. The focal plane, which is where the science detector is located, shows the Fourier transform of the pupil plane, which is where the deformable mirror (DM) is located. A sine wave on the DM generates delta functions (PSFs) on the science detector. This is shown in Figure 1. The amplitude, phase, orientation, and frequency of the sine wave on the DM determines the brightness, phase, location, and spacing of the artificial speckles on the science detector. Because the speckle halo is starlight that has been scattered away from the PSF core, it is coherent with the artificial speckles produced with this technique. Therefore, one can generate an artificial speckle in the same location as an existing speckle, scan through phase to find the opposite phase, and thereby null it away. Light from an extrasolar planet is not coherent with starlight, so it cannot be nulled away. In practice, this worked well on the SCEXAO internal light source, but because it collected images at ~ 170 Hz and required many phase measurements per iteration, it was not fast enough to affect the dynamic speckles when tested on-sky.

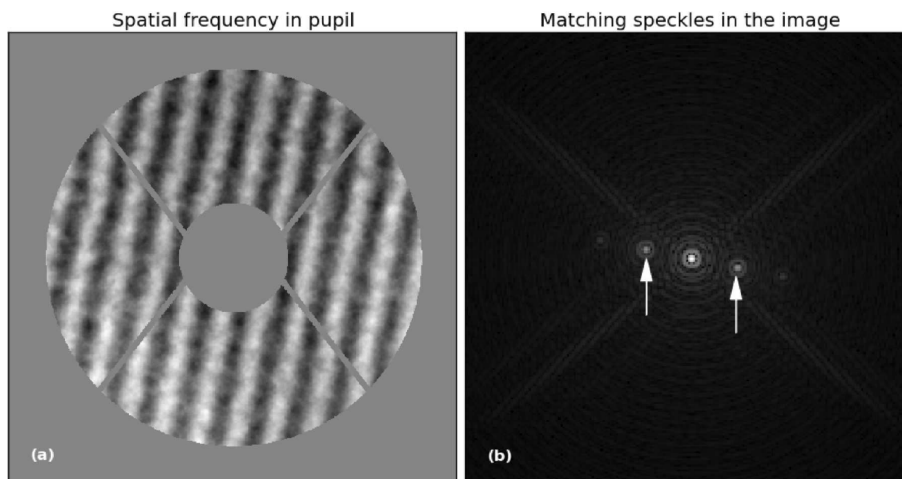


Figure 1. On the left is a map of deformable mirror displacement, and on the right are the resulting speckles produced in the focal plane. By varying the orientation, frequency, amplitude, and phase of the sine wave on the DM, one varies the location, spacing, brightness, and phase of the artificial speckles, respectively. Multiple sine waves can be applied in order to produce multiple speckles. Figure reproduced from Martinache et al. 2014.⁶

SCEXAO^{7,8} (Subaru Coronagraphic Extreme Adaptive Optics) is an instrument at Subaru Telescope atop Maunakea in Hawaii. It utilizes a pyramid wavefront sensor and 2000-element DM updating at typically 2 kHz. AO188,⁹ Subaru’s facility AO system, provides preliminary corrections, and then SCEXAO provides high-order corrections in order to achieve Strehls of 80-90% at H band. SCEXAO is intended to observe high-contrast objects such as extrasolar planets, brown dwarfs, and debris disks. Numerous different modules can utilize SCEXAO’s corrected beam. Visible light is sent to the VAMPIRES¹⁰ and FIRST¹¹ aperture-masking interferometers. Infrared light can be directed to the CHARIS integral field spectrograph,¹² HiCIAO imager¹³ (which is being decommissioned), internal InGaAs science camera, or the SAPHIRA camera.¹⁴

SAPHIRA¹⁵ is a 320x256@24 μ m pixel HgCdTe linear avalanche photodiode detector manufactured by Leonardo. It has low dark current and noise and an adjustable gain, and it is optimized for high frame rates (up to 10 MHz per channel clocking frequencies). At bias voltages of ~ 18 V, SAPHIRA detectors have a multiplication gain of several hundred.¹⁶ Because this gain multiplies the signal but not the read noise, SAPHIRA enables the potential for photon-counting performance.¹⁷ SAPHIRA detectors have 32 outputs; unlike HAWAII detectors, these outputs are interleaved (32 adjacent pixels are read simultaneously). Reading a subarray enables proportionally higher frame rates. We operated the SAPHIRA using a Pizza Box controller developed at the University of Hawaii Institute for Astronomy.

2.2 Observations

On the nights of May 31, August 13, and August 15, 2017, we recorded SAPHIRA images of unresolved stars. Datasets were collected with SCEXAO+AO188 (extreme adaptive optics) corrections, AO188 corrections only, and with no adaptive optics. In each regime, approximately one minute of data was collected with each of a 10nm bandpass filter centered at H, a 50nm bandpass filter centered at H, and a full H filter (about 260nm bandpass). The narrower bandpass filters enabled better resolving of the speckles because they reduced chromatic elongation. The data presented in this paper utilized the 50nm bandpass filters. The three bandpasses in each of the three AO regimes produced nine datasets per night. The detector was subwindowed to 128x128 pixels (approximately a 1 arcsecond square) in order to achieve a frame rate of 1.68 kHz. The PSF core was saturated by a factor of ~ 10 in order to obtain better SNR for the speckles.

In order to align images and provide a flux calibration, we applied an astrometric grid¹⁸ during observations. In short, sine waves in orthogonal directions with frequencies optimized to the DM actuator pitch were applied to the DM. This generated an artificial speckle in each corner of the detector. By alternating the phase of the sine waves between 0 and π on timescales shorter than individual SAPHIRA exposures, the astrometric speckles became effectively incoherent with the speckle halo. This avoided potential interference between the artificial and natural speckles that could distort the position and lifetime measurements.

The SAPHIRA detector was operated in “read-reset” mode, wherein each line was read once and then reset. This enabled a maximum effective frame rate, optimal duty cycle, and full use of the dynamic range per image. We later collected dark/bias frames and subtracted these in order to remove the detector’s fixed-pattern noise. In our previous speckle lifetime measurements,¹⁹ we operated the detector in up-the-ramp mode (multiple reads followed by a reset) and then subtracted adjacent reads. This resulted in irregular time sampling and much poorer SNR due to having to split the flux over multiple reads. Additionally, in the previous observations, we did not have the astrometric grid available for aligning images in post-processing, so we did not saturate the PSF core during observations. For these reasons, our more recent observations are much higher quality than the older ones.

3. ANALYSIS

3.1 Data Reduction

Our goal is to see how speckles evolve as a function of time and brightness. Given that tip/tilt of the PSF would cause a change in brightness at a pixel not due to speckle evolution, we began by aligning all the images. The results of the image alignment are shown in Figure 2. We located the astrogrid speckles and aligned images using those, and as a check also cross-correlated each image against the next to detect shifts. Both techniques registered images to ~ 0.01 pixel accuracy and produced similar results. Second, we selected all pixels within a radius of $4\lambda/D < r < 10\lambda/D$ of the PSF core. Given that intensity I goes as the square of complex amplitude A ,

$$I \sim |A|^2 \tag{1}$$

it follows that

$$\frac{dI}{dt} \sim 2A \frac{dA}{dt} \tag{2}$$

and therefore brighter speckles will change more quickly than dimmer ones. Because of this, we sorted the pixels into brightness bins (we selected the 20-30 percentile brightness pixels, 40-50 percentile, etc.). For each selection

of pixels, we subtracted those pixels from the same pixels time t later. This formed a difference image. Finally, we calculated the spatial standard deviation in order to measure how the pixels have changed in brightness over that time interval. We repeated this process for each image relative compared to 1-260 frames later, so thousands of measurements were averaged to improve sensitivity. We plotted the standard deviation against time for each wavelength bin, as is shown in Figures 3 (extreme AO, AO188 only, and no AO on the night of May 31, 2017) and 4 (the extreme AO plots for August 13 and 15, 2017).

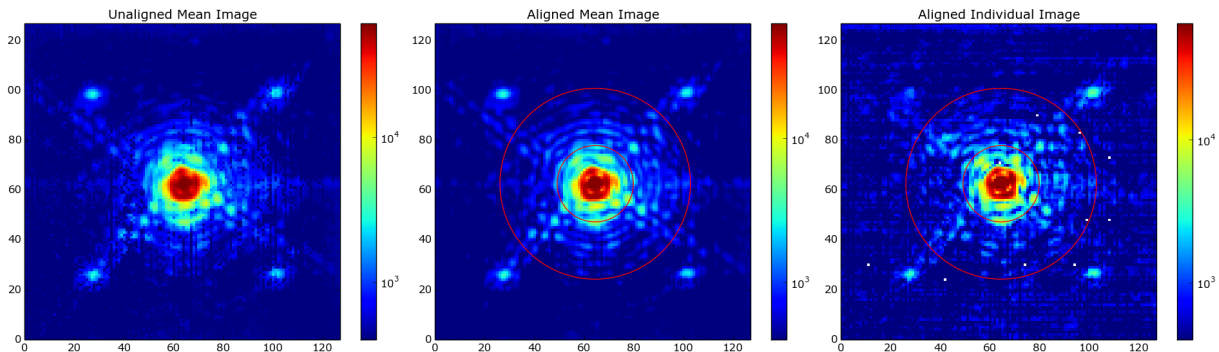


Figure 2. Shown are three sample logarithmically scaled ExAO-corrected PSFs from the May 31, 2017 dataset. The four bright speckles in the corners are the artificial astrometric speckles we created for alignment (the PSF core couldn't be used because it was saturated). Overplotted on the second and third images are circles indicating $r = 4\lambda/D$ and $r = 10\lambda/D$ (the region within which we analyzed speckle lifetimes). The left image shows the result of coadding 10,000 frames (6 seconds of data), and the middle one is the same images coadded after being aligned. Due to the alignment, the middle image exhibits many more airy rings and better-defined speckles than the left one. Tip-tilt errors consistently are the dominant source of Strehl reduction for SCEXAO corrections. The right image is a sample individual frame. One astrometric speckle is much dimmer due to a rolling shutter effect.

3.2 Work to be Done: Interpreting the Speckle Behavior

One could fit a line to the extreme AO plots in Figures 3 or 4 and solve for a given contrast as a function of time. This would provide the loop update rate that would be necessary to stabilize the speckle halo to that contrast level, and this is what we did in our 2016 paper. However, we have not done that yet because we are concerned that our speckle analysis contains a systematic effect that we have not accounted for. Since intensity scales as the square of complex amplitude as stated in Equation 1, and on short timescales the complex amplitude changes linearly, therefore intensity should increase with an upward parabolic behavior on short timescales. However, our data appears linear or perhaps parabolic with negative concavity. This is not the behavior that we would expect, and we are currently investigating this. Therefore the results shown in this paper should be considered preliminary.

4. CONCLUSIONS

We collected H-band images of the speckle halo surrounding the SCEXAO PSF at a framerate of 1.68 kHz. We then reduced the data in order to see how speckles evolve as a function of time and brightness. We are currently in the process of analyzing the results in order to predict the effectiveness of a real-time speckle nulling loop. Once we complete this process (hopefully in the next half year), we will submit a follow-up publication.

A low-speed (\sim couple Hz bandwidth) speckle nulling loop was implemented by Martinache⁶ in 2014 on SCEXAO using the instrument's (comparatively noisy) InGaAs camera, but we are interested in utilizing the high frame rate and sensitivity of SAPHIRA or MKIDs to implement a more optimized version in the future. In combination with post-processing techniques such as spectral differential imaging, these speckle reduction methods will enable the detection of ultra-high-contrast subjects such as reflected light extrasolar planets.

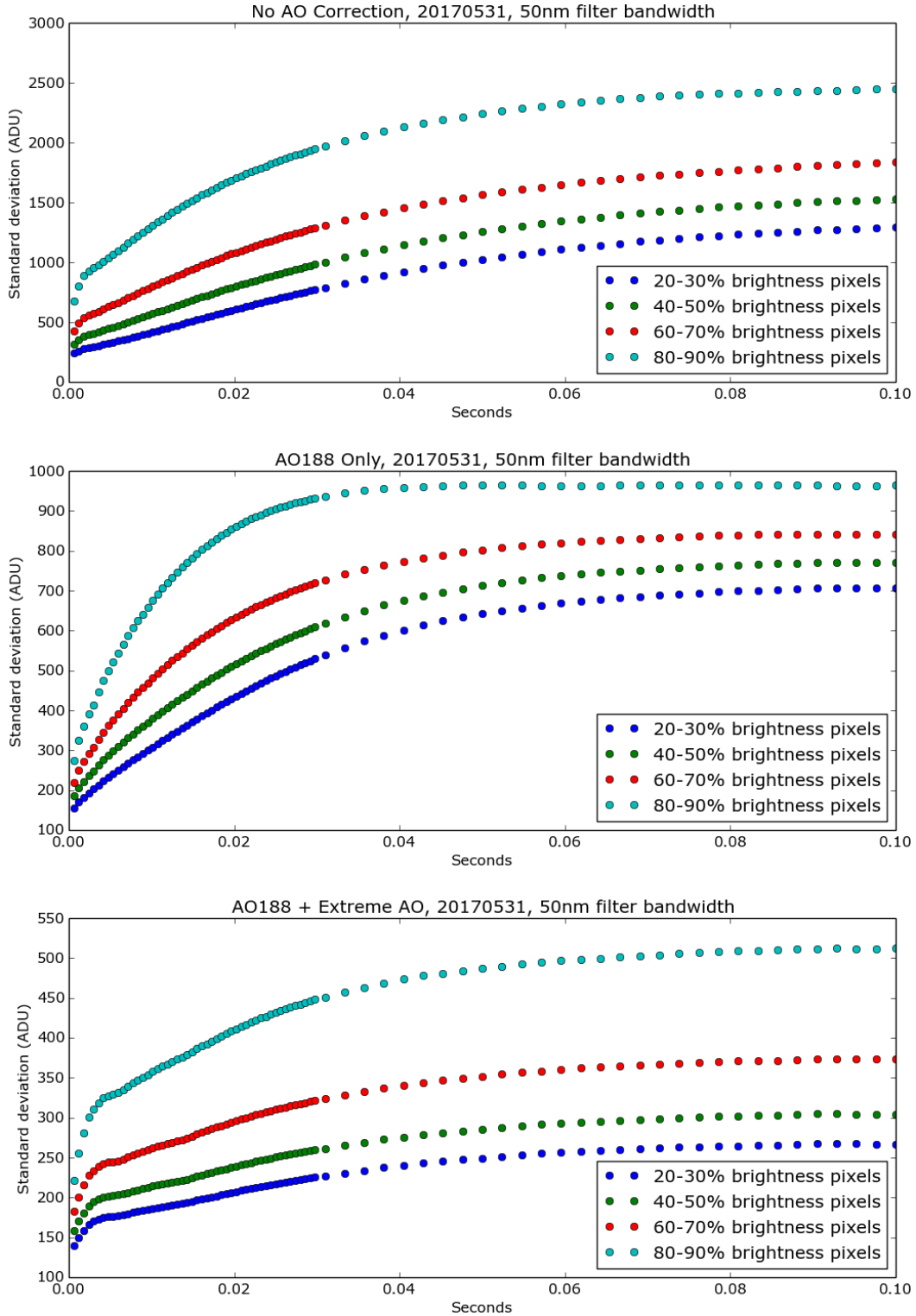


Figure 3. Shown here are the speckle evolution plots for four different brightness bins and the three different AO regimes (no AO, AO188 only, and AO188+extreme AO) on the night of May 31, 2017. AO188 corrections reduce the standard deviation in speckle brightness relative to having no AO, and ExAO again reduces it relative to AO188. The plots approach asymptotic values because the speckles have entirely changed after some amount of time. The time sampling becomes coarser after ~ 0.03 seconds in order to reduce the computational processing time to produce these plots.

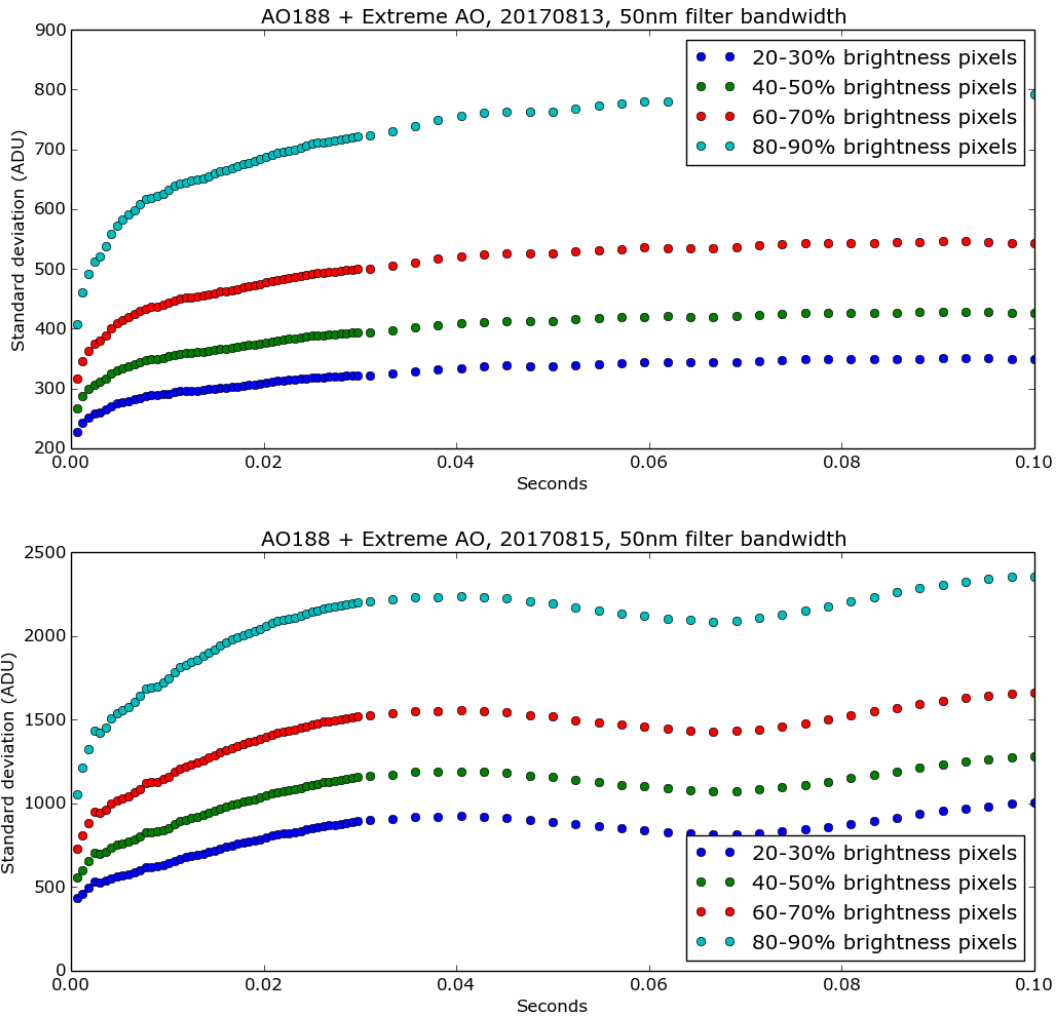


Figure 4. These two plots are equivalent to the bottom plot in Figure 3, but were produced using the extreme AO data collected on August 13 (top) and 15 (bottom), 2017. The seeing and AO tuning were significantly different in each of the three nights. Due to differing flux levels, the three epochs of data have different vertical offsets. The time sampling becomes sparser after ~ 0.03 seconds in order to reduce the computational processing time to produce these plots.

ACKNOWLEDGMENTS

The authors acknowledge support from NSF award AST 1106391, NASA Roses APRA award NNX 13AC14G, and the JSPS (Grant-in-Aid for Research #23340051 and #26220704).

REFERENCES

- [1] Macintosh, B., Poyneer, L., Sivaramakrishnan, A., and Marois, C., “Speckle lifetimes in high-contrast adaptive optics,” in [*Astronomical Adaptive Optics Systems and Applications II*], Tyson, R. K. and Lloyd-Hart, M., eds., *Proc. SPIE* **5903**, 170–177 (Aug. 2005).
- [2] Marois, C., Lafrenière, D., Doyon, R., Macintosh, B., and Nadeau, D., “Angular Differential Imaging: A Powerful High-Contrast Imaging Technique,” *ApJ* **641**, 556–564 (Apr. 2006).
- [3] Smith, W. H., “Spectral differential imaging detection of planets about nearby stars,” *PASP* **99**, 1344–1353 (Dec. 1987).
- [4] Malbet, F., Yu, J. W., and Shao, M., “High-Dynamic-Range Imaging Using a Deformable Mirror for Space Coronagraphy,” *PASP* **107**, 386 (Apr. 1995).
- [5] Give’On, A., Kasdin, N. J., Vanderbei, R. J., and Avitzour, Y., “On representing and correcting wavefront errors in high-contrast imaging systems,” *Journal of the Optical Society of America A* **23**, 1063–1073 (May 2006).
- [6] Martinache, F., Guyon, O., Jovanovic, N., Clergeon, C., Singh, G., and Kudo, T., “On-sky speckle nulling with the Subaru Coronagraphic Extreme AO (SCEXAO) instrument,” in [*Society of Photo-Optical Instrumentation Engineers (SPIE) Conference Series*], *Society of Photo-Optical Instrumentation Engineers (SPIE) Conference Series* **9148**, 21 (Aug. 2014).
- [7] Jovanovic, N., Guyon, O., Martinache, F., Clergeon, C., Singh, G., Vievard, S., Kudo, T., Garrel, V., Norris, B., Tuthill, P., Stewart, P., Huby, E., Perrin, G., and Lacour, S., “SCEXAO as a precursor to an ELT exoplanet direct imaging instrument,” in [*Proceedings of the Third AO4ELT Conference*], Esposito, S. and Fini, L., eds., 94 (Dec. 2013).
- [8] Jovanovic, N., Guyon, O., Lozi, J., Currie, T., Hagelberg, J., Norris, B., Singh, G., Pathak, P., Doughty, D., Goebel, S., Males, J., Kuhn, J., Serabyn, E., Tuthill, P., Schworer, G., Martinache, F., Kudo, T., Kawahara, H., Kotani, T., Ireland, M., Feger, T., Rains, A., Bento, J., Schwab, C., Coutts, D., Cvetojevic, N., Gross, S., Arriola, A., Lagadec, T., Kasdin, J., Groff, T., Mazin, B., Minowa, Y., Takato, N., Tamura, M., Takami, H., and Hayashi, M., “The SCEXAO high contrast imager: transitioning from commissioning to science,” in [*Adaptive Optics Systems V*], *Proc. SPIE* **9909**, 99090W (July 2016).
- [9] Minowa, Y., Hayano, Y., Oya, S., Watanabe, M., Hattori, M., Guyon, O., Egner, S., Saito, Y., Ito, M., Takami, H., Garrel, V., Colley, S., Golota, T., and Iye, M., “Performance of Subaru adaptive optics system AO188,” in [*Society of Photo-Optical Instrumentation Engineers (SPIE) Conference Series*], *Society of Photo-Optical Instrumentation Engineers (SPIE) Conference Series* **7736**, 3 (July 2010).
- [10] Norris, B., Schworer, G., Tuthill, P., Jovanovic, N., Guyon, O., Stewart, P., and Martinache, F., “The VAMPIRES instrument: imaging the innermost regions of protoplanetary discs with polarimetric interferometry,” *MNRAS* **447**, 2894–2906 (Mar. 2015).
- [11] Huby, E., Perrin, G., Marchis, F., Lacour, S., Kotani, T., Duchêne, G., Choquet, E., Gates, E. L., Woillez, J. M., Lai, O., Fédou, P., Collin, C., Chapron, F., Arslanyan, V., and Burns, K. J., “FIRST, a fibered aperture masking instrument. I. First on-sky test results,” *A&A* **541**, A55 (May 2012).
- [12] Groff, T. D., Chilcote, J. K., Kasdin, J., Brandt, T., Galvin, M., Loomis, C., Carr, M., Knapp, G. R., Guyon, O., Jovanovic, N., Lozi, J., Takato, N., and Hayashi, M., “On-Sky Performance Verification of the CHARIS IFS,” in [*American Astronomical Society Meeting Abstracts*], *American Astronomical Society Meeting Abstracts* **229**, 155.10 (Jan. 2017).
- [13] Hodapp, K. W., Suzuki, R., Tamura, M., Abe, L., Suto, H., Kandori, R., Morino, J., Nishimura, T., Takami, H., Guyon, O., Jacobson, S., Stahlberger, V., Yamada, H., Shelton, R., Hashimoto, J., Tavrov, A., Nishikawa, J., Ukita, N., Izumiura, H., Hayashi, M., Nakajima, T., Yamada, T., and Usuda, T., “HiCIAO: the Subaru Telescope’s new high-contrast coronagraphic imager for adaptive optics,” in [*Society of Photo-Optical Instrumentation Engineers (SPIE) Conference Series*], *Society of Photo-Optical Instrumentation Engineers (SPIE) Conference Series* **7014**, 19 (July 2008).

- [14] Atkinson, D., Hall, D., Baranec, C., Baker, I., Jacobson, S., and Riddle, R., “Observatory deployment and characterization of SAPHIRA HgCdTe APD arrays,” in [*Society of Photo-Optical Instrumentation Engineers (SPIE) Conference Series*], *Society of Photo-Optical Instrumentation Engineers (SPIE) Conference Series* **9154**, 19 (July 2014).
- [15] Finger, G., Baker, I., Alvarez, D., Ives, D., Mehrgan, L., Meyer, M., Stegmeier, J., and Weller, H. J., “SAPHIRA detector for infrared wavefront sensing,” in [*Adaptive Optics Systems IV*], *Proc. SPIE* **9148**, 914817 (Aug. 2014).
- [16] Atkinson, D. E., Hall, D. N. B., Baker, I. M., Goebel, S. B., Jacobson, S. M., Lockhart, C., and Warmbier, E. A., “Next-generation performance of SAPHIRA HgCdTe APDs,” in [*High Energy, Optical, and Infrared Detectors for Astronomy VII*], *Proc. SPIE* **9915**, 99150N (Aug. 2016).
- [17] Finger, G., Baker, I., Alvarez, D., Dupuy, C., Ives, D., Meyer, M., Mehrgan, L., Stegmeier, J., and Weller, H. J., “Sub-electron read noise and millisecond full-frame readout with the near infrared eAPD array SAPHIRA,” in [*Adaptive Optics Systems V*], *Proc. SPIE* **9909**, 990912 (July 2016).
- [18] Jovanovic, N., Guyon, O., Martinache, F., Pathak, P., Hagelberg, J., and Kudo, T., “Artificial Incoherent Speckles Enable Precision Astrometry and Photometry in High-contrast Imaging,” *ApJ* **813**, L24 (Nov. 2015).
- [19] Goebel, S. B., Guyon, O., Hall, D. N. B., Jovanovic, N., and Atkinson, D. E., “Evolutionary timescales of AO-produced speckles at NIR wavelengths,” in [*Adaptive Optics Systems V*], *Proc. SPIE* **9909**, 990918 (July 2016).